International Journal of Nanomedicine

Dovepress
open access to scientific and medical research

Open Access Full Text Article

ORIGINAL RESEARCH

Spray-Dried Silica Xerogel Nanoparticles as a Promising Gastroretentive Carrier System for the Management of Chemotherapy-Induced Nausea and Vomiting

This article was published in the following Dove Press journal:
International Journal of Nanomedicine

Amira Mohsen Ghoneim[1]
Mina Ibrahim Tadros[2]
Ahmed Adel Alaa-Eldin[3]

[1]Department of Pharmaceutics and Pharmaceutical Technology, Faculty of Pharmaceutical Sciences and Pharmaceutical Industries, Future University in Egypt (FUE), New Cairo, Egypt; [2]Department of Pharmaceutics and Industrial Pharmacy, Faculty of Pharmacy, Cairo University, Cairo, Egypt; [3]Department of Pharmaceutics, College of Pharmaceutical Sciences and Drug Manufacturing, Misr University for Science & Technology (MUST), 6th of October City, Egypt

Purpose: The current work aimed to develop spray-dried silica xerogel nanoparticles (SXNs) as a gastroretentive carrier for the dual delivery of chlorambucil (CHL) and granisetron hydrochloride (GR). As a low-density system, it was proposed to float over gastric fluids; allowing for the retention of CHL in the acidic medium where it is more stable while ensuring the solubility of GR.

Methods: Silica xerogels were developed by sol-gel process, using Tetraethyl orthosilicate (TEOS) water and acetic acid, followed by spray drying. SXNs were evaluated for particle size, zeta potential, entrapment efficiency (EE%), CHL and GR release after 1 hr (P_{1h}) and after 8 hrs (P_{8h}). The best achieved system (SXN4) was evaluated for morphology, pore diameter, total porosity, bulk density, wetting time, floating characteristics. Furthermore, the pharmacokinetics of the loaded drugs were evaluated in rats; relative to an aqueous CHL suspension containing GR.

Results: SXN4 system had the highest desirability (0.69); showing spherical nanoparticles (181.63 nm), negative zeta potential (−5.18 mV), promising EE% of 59.39% and 73.94% (for CHL and GR, respectively) and sustained CHL and GR release profiles characterized by low P_{1h} (22.75% and 30.74%) and high P_{8h} (60.36% and 99.33%), respectively. It had a mean pore diameter of 8.622 nm, a total porosity of 62.27%, a bulk density of 0.605 g/mL, a wetting time of 292 sec, zero lag time and a floating duration of at least 8 h.

Conclusion: The prolongation in the mean residence time ($MRT_{(0-\infty)}$) and the promotion of the relative oral bioavailabilities of both drugs could unravel the potential of this system for the management of chemotherapy-induced nausea and vomiting.

Keywords: chlorambucil, granisetron hydrochloride, silica xerogel nanoparticles, low density, gastroretentive

Introduction

Chlorambucil (CHL) is a synthetic derivative of nitrogen mustard. It acts as a cell cycle phase-nonspecific DNA alkylating agent. It has been prescribed in the palliative treatment to patients of chronic lymphocytic leukemia, malignant lymphomas including giant follicular lymphoma, lymphosarcoma, and Hodgkin's disease, and other forms of cancer.[1] It is commercially available as 2 mg oral tablets. The usual oral daily dosage for the average patient usually ranges from 4 to 10 mg per day. It should be taken on an empty stomach since food reduces drug

Correspondence: Mina Ibrahim Tadros
Department of Pharmaceutics and Industrial Pharmacy, Faculty of Pharmacy, Cairo University, Kasr El-Aini St, Cairo 11562, Egypt
Tel +002-01223620458
Email mina.tadros@pharma.cu.edu.eg; mina_ebrahim@yahoo.com

submit your manuscript | www.dovepress.com
DovePress
http://doi.org/10.2147/IJN.S232841

bioavailability. As a nitrogen mustard-member, CHL suffer from certain drawbacks following oral administration, including; the rapid hydrolysis of the chloroethyl group in neutral to basic aqueous media,[2] the limited therapeutic efficacy and the significant intra- and inter-subject variations in drug pharmacokinetics.[2,3] The latter problems were related to its short elimination half-life in plasma (1–2 h) and its limited water solubility.[4] Although CHL's degree of emetogenicity is considered low, a high potential to induce nausea and vomiting usually occur with high doses and/or during multiday chemotherapy.[5,6] Not only does this influence the patients compliance towards chemotherapeutics, but also influences their quality of life and/or their decision in continuing the treatment protocol.[7,8]

Granisetron hydrochloride (GR) is the drug of choice in the control of chemotherapy-induced emesis in the first 24h post-chemotherapy (acute emesis).[9] It is a potent serotonin 5-HT3 receptor antagonist which inhibits the activity of the vagus nerve, responsible for activation of the vomiting center found in the medulla oblongata.[10] GR is a hydrophilic dug which possess a short half-life of 3 to 4 h in healthy volunteers and of 9 to 12 h in patients with cancer. Following oral administration (2 mg daily), it suffers from a limited bioavailability (60%) due to the hepatic first pass metabolism.[11,12]

Traditional chemotherapy regimens typically adopt the maximal tolerated drug dose to kill as many cancer cells as possible. Consequently, definite cycle breaks are needed to allow recovery from the side effects. Unfortunately, these interruptions can promote tumor re-growth with a possibility of developing drug-resistant cancer cells.[13] Therefore, metronomic chemotherapy was introduced to allow exposure of the tumor to a low dose of the chemotherapeutic drug on an almost continuous basis.[1,14] This regimen should be carefully designed so as not to provide prolonged drug-free intervals which may cause tumor re-growth. Meanwhile, it should prevent the drug plasma level from exceeding the maximum tolerable concentration, so as to control the drug adverse effects.[15] Porous carriers, like silica nanoparticles, can be used for metronomic chemotherapy and targeting drug(s) to specific tumors in the body, thus resulting in a higher efficacy and reduced adverse events.[16] The drug-loading capability, particle size, morphology, pore size and structure can be tailored for targeting high amounts of therapeutic agents, with minimal in-vivo degradation.[17] Furthermore, the sol–gel processed silica xerogel nanoparticles have the intrinsic promising advantages, including the good mechanical properties, the high chemical, thermal and electrical stability, and a favorable tissue response.[18] Cancer cells expressing caveolin-1 are more likely to endocytose silica nanoparticles before being transferred to lysosomes; allowing for the release of the loaded drug(s).[19,20]

The current work aimed to develop a promising gastroretentive system loaded with CHL and GR, using silica nanoparticles as a targeting carrier, via spray drying. This system is expected to overcome most of the limitations of CHL and improve its oral bioavailability by keeping it at the stomach where it is more stable at pH values < 2.[21] Furthermore, the achievement of a promising sustained release profile of CHL would be expected to improve the patient compliance by minimizing the frequency of drug administration. On the other hand, gastroretentive systems are of particular interest for basic drugs, like GR, which are poorly soluble at the alkaline pH of the intestine and hence, could be expected to improve their oral bioavailabilities.

Materials and Methods

Materials

Chlorambucil (CHL), acetonitrile (HPLC grade), phosphoric acid (HPLC grade), methanol (HPLC grade), ammonium formate (HPLC grade), formic acid (HPLC grade) and Lamivudine (internal standard) were purchased from Sigma-Aldrich Chemical Co. (St. Louis, MO). Granisetron hydrochloride (GR) was kindly provided by Amoun Pharmaceutical Co. (Cairo, Egypt). Tetraethyl orthosilicate (TEOS) was obtained from Merck Millipore (Darmstadt, Germany). Glacial acetic acid and concentrated hydrochloric acid were purchased from El-Nasr pharmaceutical chemicals Co. (Cairo, Egypt). Spectra/Pore® dialysis membrane (molecular weight cut off; 12–14 kDa) was derived from Spectrum Laboratories Inc. (Rancho Dominguez, CA).

Preparation of (GR/CHL)-Loaded Spray Dried Silica-Xerogel Nanoparticles (SXNs)

Silica sol containing CHL and GR was simply developed in a two-step sol-gel process.[22] After the complete hydrolysis of Tetraethyl orthosilicate (TEOS), in the presence of acetic acid as a catalyst, has propagated till a homogenous clear sol is formed, CHL (4 mg) and GR (2 mg) were added directly to the sol and left for one hour in an incubator shaker (IKA® KS 4000 i-control orbital shaker, Staufen im Breisgau, Germany) to ensure complete solubilization of the drugs in the sol. The loaded sol system was spray dried using a Büchi 190 nozzle-type mini-spray dryer (Flawil, Switzerland) to

develop (GR/CHL)-loaded spray dried silica xerogel nanoparticles (SXNs). Based on the results of the preliminary studies, the following parameters were explored in the spray drying process so as to develop promising nanoparticles as well as to minimize the loss of spray dried powders on the outlet walls of the drying chamber; without influencing their flowability and/or floating characteristics. The flow rate (using a peristaltic pump) was 5 mL/min; the inlet and outlet temperatures were 125°C and 80°C, respectively; the air pressure of the spray was 4 kg/cm^2, and the diameter of the nozzle was 0.7 mm.

Design of Experiments (DoE)

The response surface design was adopted to study the effect of two independent variables at three levels on seven responses. The variables were the molar ratio of water (15, 20, and 25) and the molar ratio of acetic acid (0.5, 1 and 1.5), while the molar ratio of TEOS was fixed at 1. The responses were the particle size, the entrapment efficiency percentage (EE%) of each drug and the released percentage of each drug after 1 h (P_{1h}) and after 8 h (P_{8h}). Thirteen experimental runs were designed for nine investigated systems using Minitab Statistical Software (Minitab® 17, State College, PA) following the central composite design; Table 1. The central point was repeated to minimize experimental error.

Characterization of (GR/CHL)-Loaded SXNs

Assessment of Particle Size, Polydispersity Index and Zeta Potential

(GR/CHL)-loaded SXNs were appropriately diluted with water and the particle size, zeta potential and the polydispersity index (PDI) of the resulting dispersions were measured with Zetasizer (Malvern-ZEN® 3600, Worcestershire, UK), at 25°C, by photon correlation spectroscopy. This technique analyzes the fluctuation in light scattering due to the Brownian motion of the particles as function of time. Light scattering was monitored at a 90º angle.[4]

Estimation of GR and CHL Entrapment Efficiency Percentages

The EE% of GR and CHL in SXNs was determined indirectly by assessment of the unentrapped drug concentrations. The SXNs dispersions were centrifuged at 15,000 rpm (1 h; 4°C) (Heraeus Megafuge® 1.0 R; Hanau, Germany) and the clear supernatants were diluted. Free GR and CHL concentrations were assessed via in-house developed and validated stability indicating assay using Shimadzu HPLC system (Kyoto,

Table 1 The Composition (Molar Ratio) and the Physicochemical Properties of the Investigated (GR/CHL)-Loaded Spray Dried SXNs (Mean ± S.D., n = 3)

System	TEOS: Water: Acetic Acid (Molar Ratio)	Physicochemical Properties			CHL			GR			Desirability Values
		Size (nm)	PDI	Zeta Potential (mV)	EE (%)	P_{1h} (%)	P_{8h} (%)	EE (%)	P_{1h} (%)	P_{8h} (%)	
SXN1	1:15:0.5	143.80 ± 6.71	0.13 ± 0.02	−5.59 ± 0.22	42.16 ± 1.94	15.23 ±2.10	53.97 ± 6.12	72.15 ± 1.94	19.08 ± 5.21	93.25 ± 5.20	0.62
SXN2	1:15:1.0	211.81 ± 16.19	0.18 ± 0.01	−5.23 ± 0.14	45.10 ± 0.39	21.04 ± 6.31	64.14 ± 4.21	70.46 ± 0.16	27.89 ± 6.22	98.80 ± 4.41	0.61
SXN3	1:15:1.5	465.41 ± 36.91	0.35 ± 0.06	−5.25 ± 0.34	52.47 ± 1.54	20.14 ± 4.24	64.16 ± 6.24	69.83 ± 3.16	30.24 ± 8.25	98.06 ± 3.14	0.36
SXN4	1:20:0.5	181.63 ± 7.82	0.22 ± 0.03	−5.18 ± 0.34	59.39 ± 1.97	22.75 ± 7.57	60.36 ± 5.19	73.94 ± 1.58	30.74 ± 9.34	99.33 ± 1.47	0.69
SXN5	1:20:1.0	242.66 ± 17.82	0.24 ± 0.01	−3.10 ± 0.19	62.17 ± 2.35	27.14 ± 9.70	69.38 ± 7.46	71.49 ± 0.29	36.24 ± 6.19	98.36 ± 1.97	0.64
SXN6	1:20:1.5	502.43 ± 19.45	0.48 ± 0.04	−4.27 ± 0.20	57.17 ± 1.93	30.97 ± 6.25	73.25 ± 6.49	74.50 ± 1.38	39.47 ± 7.91	98.87 ± 4.71	0.36
SXN7	1:25:0.5	127.45 ± 13.52	0.14 ± 0.04	−4.89 ± 0.74	71.67 ± 1.38	35.95 ± 6.93	60.58 ± 5.18	82.42 ± 2.18	40.97 ± 9.31	98.70 ± 3.13	0.64
SXN8	1:25:1.0	141.82 ± 9.56	0.28 ± 0.06	−4.97 ± 0.94	69.41 ± 1.42	38.71 ± 8.12	72.00 ± 4.59	84.57 ± 1.74	51.61 ± 9.50	99.07 ± 2.12	0.51
SXN9	1:25:1.5	347.16 ± 15.23	0.42 ± 0.07	−5.17 ± 0.64	72.87 ± 0.82	49.13 ± 5.69	85.18 ± 3.16	87.18 ± 0.98	60.24 ± 8.66	99.70 ± 1.56	0.22

Japan) at a detection wavelength of 254 nm. The mobile phase consisted of 80% phosphoric acid (0.2%, v/v) and 20% acetonitrile. The isocratic flow rate was 1mL/min while the stroke volume was 150 µL. The separation of the drugs was performed on YMC-Pack Pro C_8 column (3 µm, 120 Å, 12 nm, 100 x 4.6 mm).

The EE% was calculated using equation (1);

$$\%\,EE = \frac{\text{Total theoretical amount of drug (mg)} - \text{Amount of unentrapped drug (mg)}}{\text{Total theoretical amount of drug (mg)}} \times 100 \quad (1)$$

In-vitro Release Studies of GR and CHL

The release studies of each drug were conducted, in triplicates, in USP Dissolution Tester (Vision® G2 Elite 8™) type II. The paddles rotated at a speed of 50 rpm. The studies were conducted in 0.1N HCl (100 mL, 37 ±0.5°C) using the bulk-equilibrium reverse dialysis technique.[23,24] Eight dialysis bags, each containing 5 mL aliquots of 0.1N HCl, were left to equilibrate in the dissolution medium within each dissolution flask for 12 h prior to experiments. On the study day, samples of (GR/CHL)-loaded SXNs were directly placed into the dissolution flasks. One dialysis bag was withdrawn at each predetermined time interval and the dissolution medium was restocked to maintain sink conditions.[25] The contents of GR and CHL in each aliquot were analyzed via HPLC; as previously described. The released percentages of CHL and GR were plotted versus time for each system. The released percentages of each drug after 1 h (P_{1h}) and after 8 h (P_{8h}) were determined. Parallel experiments were conducted using an aqueous suspension of CHL (4 mg/mL) and an aqueous solution of GR (2 mg/mL).

Selection of the Best Achieved (GR/CHL)-Loaded SXN

The data were analyzed using Minitab® 17 software to determine the optimum conditions and elaborate the system possessing the highest desirability value; with respect to seven constraints. The particle size of SXN and P_{1h} of each drug were desired to be at minimum values while the EE% and P_{8h} of each drug were aimed to achieve maximum values. Based on the proposed importance of these constraints, the response weight values of the particle size of SXN and P_{1h} of each drug were set at 1 while those of EE% and P_{8h} of each drug were set at 0.5.

Characterization of SXN4 Possessing the Highest Desirability Value

Morphological Analysis

The topographic examination of the system was conducted using a scanning electron microscope fitted with an image analysis system (Jeol, JXA-840A, Tokyo, Japan). The system was fixed to a brass grid using double-sided adhesive tape. The sample was then sputter coated (Edwards S-150A, Crawley, England) with a layer of gold of 150 Å for 2 min in a vacuum of 3 x 10^{-1} atm of argon gas. After that, the sample was examined at 15 KV under a magnification power of X30000.

Estimation of Pore Diameter, Porosity and Density

The porosity parameters of the system were investigated via the mercury intrusion porosimetry method using PoreSizer 9320 V2.08 (Micromeritics, Norcross, GA). Several parameters were studied, including total pore surface area (A_{tot}, m^2/g), pore diameter (D, µm), mean pore diameter (D_m, µm), bulk density (P_{se}, g/mL), apparent density (P_{sa}, g/mL), and porosity (%). The pore size distribution was estimated from the plot of the incremental intrusion volumes against pore diameter (D, µm).[26]

The pore diameter was calculated according to equation 2:

$$D = \frac{-4\gamma COS\theta}{P} \quad (2)$$

where, P is the pressure (P_{sia}), γ is the surface tension of mercury (485 dyne/cm) and Θ is the contact angle (130º).[27]

The following equations (3–7) were reported by Orlu et al[28] for the calculation of the total pore surface area (A_{tot}), the mean pore diameter (D_m), the bulk density (P_{se}), the apparent density (P_{sa}) and porosity (%), as follows;

$$Atot = \frac{1}{\gamma \cos\theta}\int_0^{Vto} P.dV \times 100 \quad (3)$$

$$Dm = \frac{4Vtot}{Atot} \quad (4)$$

$$P_{se} = \frac{Ws}{Vp - VHg} \quad (5)$$

$$P_{sa} = \frac{Ws}{Vse - Vtot} \quad (6)$$

$$\text{Porosity}\,(\%) = (1 - \frac{P_{se}}{P_{se}}) \times 100 \quad (7)$$

where, V_{tot} is the total specific intrusion volume, V is the intrusion volume, V_p is the volume of empty penetrometer

(mL), V_{Hg} is the volume of mercury (mL), W_s is the weight (g) of the system and V_{se} is the volume of the empty penetrometer minus the volume of the mercury (mL).

Determination of the Wetting Time and the Floating Characteristics

The wetting time, floating lag time and floating duration of the system were estimated, in triplicate, according to the method developed by Tadros and Fahmy[26] with slight modification. The studies were conducted in USP Dissolution Tester (Vision® G2 Elite 8™) type II. The paddles rotated at a speed of 50 rpm and the testing medium was 0.1N HCl (900 mL,37 ±0.5 °C). In order to clearly visualize the propagation of the medium front throughout SXN4, methyl red (0.05%, w/v) was added to the medium to give a light pink color. The wetting time was defined as the time needed by the system to acquire a light pink color. The floating lag time was the time elapsed from introducing the system till floating to the upper one third of the medium. The floating duration was the period during which the system kept floating.

In- vivo Pharmacokinetic Studies

The aim of these studies was to estimate the pharmacokinetic parameters of CHL and GR in rats following oral administration of SXN4 (test treatment) relative to an aqueous CHL suspension containing GR (reference treatment). The protocol of the studies was approved by the Research Ethics Committee - for experimental studies - at the Faculty of Pharmacy, Cairo University (REC-FOPCU) (PT 2396) as well as the Research Ethics Committee at Faculty of Pharmaceutical Sciences and Pharmaceutical Industries, Future University in Egypt (REC-FPSPI-12/84). The guidelines of Association for Assessment and Accreditation of Laboratory Animal Care (AAALAC) were adopted.

The studies were conducted according to a two treatment, randomized, parallel design. Twelve male Wistar rats (200–220 g) were divided equally into 2 groups. The members of the first group received aliquots of (GR/CHL)-loaded SXN4 system (containing the equivalent to 2 mg GR and 4 mg CHL) while those of the second group received 1 mL samples of an aqueous CHL suspension containing GR. The latter was prepared by dissolving of GR in water followed by the addition of CHL, so that the concentration of GR and CHL would be 2 mg/mL and 4 mg/mL, respectively.

Blood aliquots were derived by puncturing the retro-orbital venous plexus, pre- (0.0 h) and post-dosing at 1.0, 2.0, 3.0, 4.0, 5.0, 6.0, 8.0, 12.0 and 24 h. The samples were collected in EDTA-loaded vials and were centrifuged at 2000×g for 10 min so that the plasma could be separated. The derived plasma samples were kept at −80 °C until analysis of loaded drugs using LC/MS/MS. The protein precipitation technique was adopted for processing of the plasma samples.[29] In brief, 0.1 mL of the samples were thawed and mixed with 0.3 mL of acetonitrile and methanol (50:50 v/v) mixture, containing the internal standard (Lamivudine, 5 µg/mL). The mixture was vortexed for 5 min then kept on ice for 30 min, followed by centrifugation to separate the proteins. Samples (20 µL) of the supernatant were injected into LC/MS/MS.

The LC/MS equipment consisted of an Agilent™ ZORBAX Eclipse Plus binary pump, an autosampler linked to a TC–C18 column (5 µm, 50 × 4.6 mm) and an Applied Biosystems Sciex Mass Spectrometer (Ontario, Canada). The oven temperature was settled at 30°C. The mobile phase consisting of a mixture of acetonitrile (80%), ammonium formate (20%) and formic acid in water (0.1%) was eluted at a flow rate of 1 mL/min. A total run time of 2 min was sufficient to allow for the simultaneous detection of CHL and GR at 1.12 and 1.03 min, respectively. The detection was performed on SCIEX Triple Quad™ 6500 tandem mass spectrometer equipped with an OptiFlow TurboV™ Electro spray ionization and heated nebulizer ionization probes. The detector was operated in the multiple reaction monitoring mode. The precursor-to-product ion transitions were m/z 303.9/192.0 for CHL and m/z 313.4/138 for GR. The respective collision energy and cone voltage for CHL and GR were 35eV and 35 V, and 16 eV and 30 V. Two calibration curves were constructed by plotting the peak area ratio of drug/IS against drug concentration in rat plasma over the concentration range of 0.05–100 ng/mL. The estimated R^2 values were 0.995 and 0.992, for CHL and GR, respectively. The procedural constants were calculated from the slopes of the curves.

Pharmacokinetic and Statistical Analyses of Data

The pharmacokinetic parameters of the test and the reference treatments were estimated for each rat. The individual plasma concentration – time curves were used for the determination of the maximum CHL and GR concentrations in rat plasma (C_{max}, ng/mL) as well as the time needed to reach C_{max} (T_{max}, h). The area under the curve from zero to 24h

($AUC_{(0-24h}$; ng.h/mL), the area under the curve from zero to infinity ($AUC_{(0-\infty)}$; ng.h/mL) and the mean residence time from zero to infinity ($MRT_{(0-\infty)}$; h) were estimated via non-compartmental analysis of data using WinNonlin® software Ver. 4.1 (Scientific consulting Inc., Cary, NC). The relative oral bioavailability of each drug was estimated from the $AUC_{(0-24h)}$ values of the test and the reference treatments.

Statistical comparison of the parametric data was performed using one-way analysis of variance (ANOVA) test at P values of <0.05. Statistical analysis on T_{max} values was performed using Mann–Whitney U-test.

Results and Discussion

Development of (GR/CHL)-Loaded SXNs

The ultimate goal of the current work was to develop a promising sustained release gastroretentive system loaded with CHL and GR, which is able to overcome most of the limitations of CHL and GR, improves their oral bioavailabilities and hence, could be effectively used in the management of chemotherapy-induced nausea and vomiting. In view of the aforementioned, TEOS-based spray dried SXNs incorporating GR and CHL were successfully prepared in a two-step sol-gel process. The latter involves the hydrolysis of TEOS (alkoxide monomers) into a colloidal solution "sol". A catalyst (acetic acid) is needed to promote the complete hydrolyses of the monomers. This process is followed by condensation, which forms an arranged network-like structure "gel"[30] After drying, the dry gel state is called "xerogel". Herein, the spray drying technique was adopted since it offers a readily scaling up technique.

The developed acid-catalyzed drug(s) loaded-sol systems were transparent and glassy. It could be inferred that the incorporation of the drugs did not change the physical characteristics of the sol systems. Yet, they were homogeneously distributed without any macroscopic phase separation and consequently, would be expected to be loaded within the spray dried silica xerogel network.[22]

For the synthesis and optimization of sol-gel processed silica nanoparticles using a mixture of TEOS, water and acetic acid, Elsagh[31] found that the developed product was very rare at low TEOS molar ratios (< 0.8). A direct correlation was observed between the TEOS molar ratio and the particle size. At an optimum TEOS molar ratio of 0.9 or 1, non-aggregated nanoparticles having uniform particle size distributions were developed.[31] These findings were in line with several reports.[32,33] Herein, a TEOS molar ratio of 1 was investigated.

Characterization of (GR/CHL)-Loaded SXNs

Assessment of Particle Size, Polydispersity Index and Zeta Potential

The particle of the investigated systems ranged from 127.45 ±13.52 nm (SXN7) to 502.43 ±19.45 nm (SXN6). The PDI values varied in the range of 0.13 ±0.02 (SXN1) to 0.48 ±0.04 (SXN6), which could indicate narrow particle size distributions; Table 1.

At a constant molar ratio of TEOS and water, a direct correlation was statistically (P< 0.05) revealed between the molar ratio of acetic acid and the mean particle size. The rate of hydrolysis and condensation increases when the concentration of the acid increases. This results in rapid creation of the initial cores, followed by crystal growth. During this condition, the fine particles aggregate and adhere forming larger ones. On the other hand, the condensation stage would be less complex at low catalyst concentrations. Consequently, the developing ionic layer around the particle would have a smaller diameter, resulting in a smaller particle size.[31]

At a constant molar ratio of TEOS and acetic acid, a direct correlation was statistically (P< 0.05) revealed between the molar ratio of water and the mean particle size. This correlation could be related to the expected increase in the rate of hydrolysis and condensation processes. This correlation was held true till a TEOS: water molar ratio of 1: 20. The further increase in the molar ratio of water lead to significant (P< 0.05) reductions in the mean particle size. This could be attributed to the activation of the hydrolytic depolymerization, which is the reverse of the condensation, in the presence of a high water content.[34]

The leaky tumor vasculature would allow the passive diffusion of particles up to 400 nm in diameter via the enhanced permeability and retention (EPR) effect.[35,36] Negatively charged nanocarriers with hydrodynamic diameter <200 nm usually undergoes slower opsonization than larger ones. This might reduce the possibility of phagocytosis and the subsequent sequestration in the spleen and the liver; resulting in a prolonged circulation time and higher accumulation in the tumor tissues.[4]

The zeta potential values of the systems were listed in Table 1. It was clear that all systems showed negative

values ranging from −3.10 ±0.19 (SXN5) to −5.59 ±0.22 (SXN1) mV. These negative charges could be related to the silanol functions formed by hydrolysis of TEOS. These results were in line with those reported by Seleem et al.[37] who developed gentamicin-loaded silica xerogel nanoparticles having zeta potential values of −1.78 and −6.24 mV.

Estimation of GR and CHL Entrapment Efficiency Percentages

The EE% of CHL varied from 42.16 ±1.94% (SXN1) to 72.87 ±0.82% (SXN9) while the EE% of GR were in the range of 69.83 ±3.16% (SXN3) to 87.18 ±0.98% (SXN9).

The high drug loading capacities of xerogel nanoparticles could be attributed to the incorporation of the drugs into the large pores of the system. Interestingly, the EE% of GR was significantly ($P< 0.05$) higher than the corresponding value of CHL within each system. The negatively charged silanol functions formed by hydrolysis of TEOS would favor the hydrogen bonding and electrostatic interactions with the positively charged GR; rather than the negatively charged CHL.

In-vitro Drug Release Studies

The in vitro release profiles of CHL and GR from GR/CHL-loaded SXNs, in comparison to an aqueous CHL suspension and an aqueous GR solution are graphically illustrated in Figures 1 and 2, respectively. It was clear that the respective P_{1h} and P_{8h} of the CHL suspension in 0.1 N HCl were ≈10 and 20% only, Figure 1.This could be partly attributed to the acidic nature of CHL and its limited solubility in water.[12] In a parallel line, one should consider the hydrolytic instability of free CHL in aqueous media; regardless of its enhanced stability in acidic aqueous media having pH values < 2.[38] The hydrolysis of chlorambucil in aqueous media involves

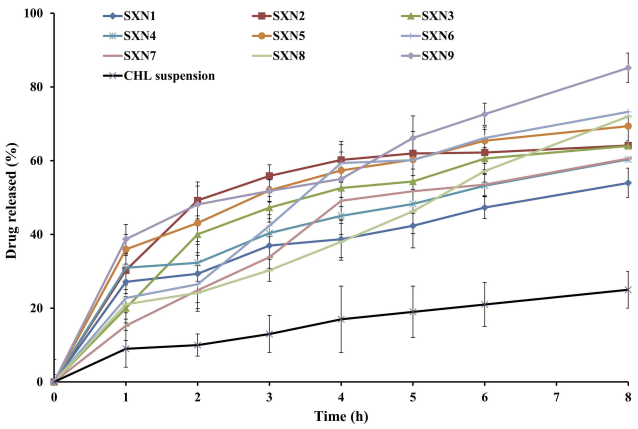

Figure 1 The in vitro release profile of CHL from SXNs, in comparison to an aqueous CHL suspension, in 0.1N HCl at 37 ± 0.5 °C (mean ± SD, n=3).

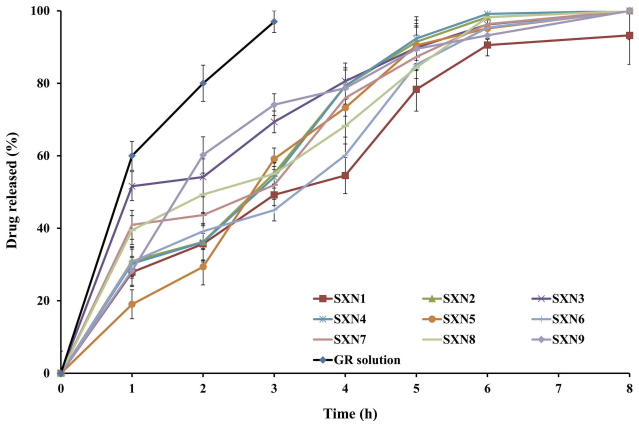

Figure 2 The in vitro release profile of GR from SXNs, in comparison to an aqueous GR solution, in 0.1N HCl at 37 ± 0.5 °C (mean ± SD, n=3).

two steps; the formation of a cationic cyclic aziridinium intermediate (the rate limiting step), and the second one involves an external aqueous nucleophilic attack. In neutral to basic aqueous media, the electron donating CHL carboxylic group could stabilize the cationic aziridinium ion; allowing for CHL hydrolysis. This occurs at a slower rate in acidic aqueous media.[2,39]

On the other hand, up to 100% of GR was released from the aqueous GR solution in 0.1 N HCl within 3 h. This could indicate a non-hindered drug diffusion via the dialysis membrane.

At a constant molar ratio of TEOS and water, a direct correlation was statistically ($P< 0.05$) revealed between the molar ratio of acetic acid and P_{1h} values of CHL and GR from SXNs. It could be inferred that the increase in the rate of hydrolysis and condensation of SXNs would promote the release of higher CHL and GR percentages. As revealed in Figures 1 and 2, the release profiles of CHL and GR from all SXNs comprised two stages; an initial burst release, followed by a slower release phase. The P_{1h} values of CHL varied from 15.23 ±2.10% (SXN1) to 49.13 ±5.69% (SXN9) while the P_{1h} values of GR varied from 19.08 ±5.21% (SXN1) to 60.24 ±8.66% (SXN9). The initial release phases could be partly attributed to the dissolution enhancing ability of silica xerogels for water insoluble drugs like CHL; due to the high surface area of these carriers[40] as well as the basic nature of GR which would favor the dissolution in acidic media. In either case, the contribution of the release of the unentrapped drug fractions and/or the release of the surface-adsorbed drug fractions should not be neglected.

The P_{8h} values of CHL varied from 53.97 ±6.12% (SXN1) to 85.18 ±3.16% (SXN9), while the P_{8h} values

of GR confirmed the almost complete release of the drug. In either case, the more prolonged release phases could be attributed to the release of the closely packed drug molecules entrapped within SXNs during the diffusion of the dissolution medium via the pores of the matrix over a prolonged period.[37]

In view of the aforementioned, it could be inferred that the incorporation of CHL in SXNs had promoted its stability in acidic aqueous media. Similar findings were reported by Wang et al[39] who related the enhanced hydrolytic stability of the adsorbed CHL in mesoporous silica microspheres to the hydrogen bonding between CHL and silica molecules and the subsequent protonation of the anionic CHL carboxylic group to the neutral form. The electron-withdrawing nature of the latter would promote the destabilization of the cationic aziridinium ion, and consequently, slowed the degradation of CHL in simulated gastrointestinal fluids over 36 h; < 10%.

The two-stage CHL release profiles are considered optimum for metronomic chemotherapy, where a tailored fraction is released during the first hour to achieve the minimum effective therapeutic concentration, followed by a sustained drug release phase to keep the drug concentration within the therapeutic window.

Based on the set constraints and the proposed weight values for particle size, EE%, P_{1h} and P_{8h} values of each drug, one system (SXN4), possessing the highest desirability value (0.69), was promoted for further characterization studies.

Characterization of SXN4

Morphological Features

The topography of the (GR/CHL)-loaded SXN4 was examined by SEM; Figure 3. Microscopic examination showed discrete spherical nanoparticles. As magnified in the inset marked in white, the presence of numerous pores and crystals of surface-adsorbed drug(s) were revealed.[41] The existence of randomly interconnected porous channels could be inferred. As proposed earlier, the contribution of the surface-adsorbed drug in the initial drug(s) release phases should not be neglected.

Estimation of Porosity, Pore Diameter, and Density

The correlation between the cumulative intrusion volume and the pore diameter of (GR/CHL)-loaded SXN4 is graphically illustrated in Figure 4. The total intrusion volume was 1.028 mL/g while the mean pore diameter was 8.622 nm. The latter value could play a role in controlling the rate

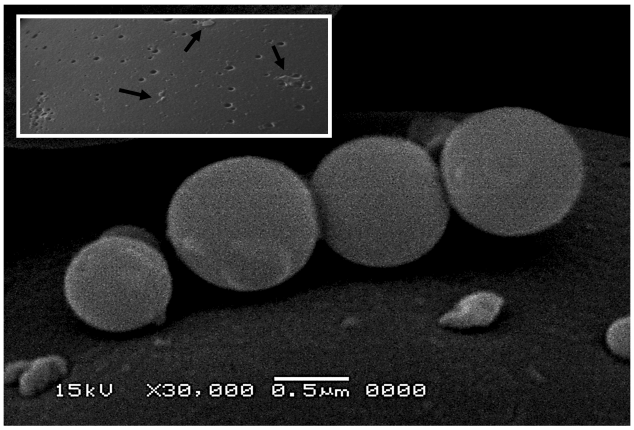

Figure 3 A scaning electron micrograph of SXN4.

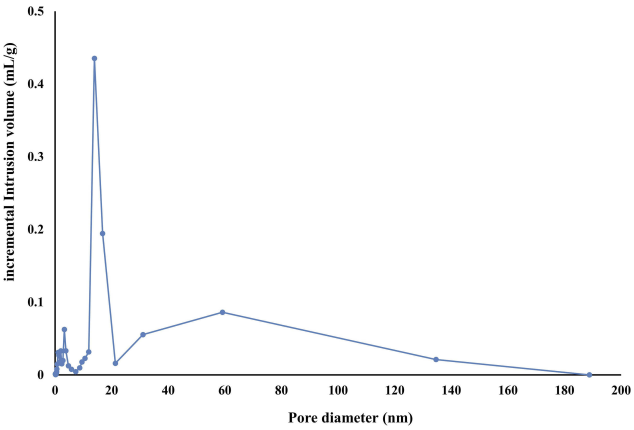

Figure 4 Pore size distribution of (GR/CHL)-loaded SXN4.

of the penetration of the dissolution medium and the subsequent release of the loaded drug(s). In a parallel line, the total pore area was 56.689 m^2/g and the total porosity percentage was 62.27%. These values could point out a unique feature of SXNs; with emphasis on those drugs possessing limited aqueous solubilities and/or hydrolytic instabilities. The bulk density of the gastric fluids ≈ 1.004 g/mL, while the estimated bulk density of SXN4 was 0.605 g/mL. Such low-density system would be expected to have excellent floating characteristics, regardless of the gastric emptying rate, over the gastric fluids for a prolonged period.[26]

The Wetting Time and Floating Characteristics

The time needed by the system to acquire a light pink color was recorded as 292 seconds. This short time could be explained with respect to the high porosity percentages and the large mean pore diameter which are expected to

allow rapid ingress of the medium. SXN4 possessed excellent floating properties with respect to their floating duration and floating lag time. The system kept floating for at least 8 hrs and had zero lag time; floated directly to the upper surface of the testing medium upon introduction; Figure 5. These findings could be attributed to the bulk density as well as the highly porous nature of this promising gastroretentive system.

In-vivo Pharmacokinetic Studies of CHL and GR in Rats

The CHL plasma concentration – time curves following oral administration of an aqueous drug suspension and SXN4 in fasted rats were depicted in Figure 6A. Remarkable differences in the shape of the drug plasma concentration-time curves between the two treatments were found; as expressed by higher C_{max} and shorter T_{max} values for CHL in SXN4. The respective C_{max} estimates from SXN4 and the aqueous suspension were 682.51 ±22.37ng/mL and 137.82 ±15.17 ng/mL, while the respective median T_{max} values were 2h and 4h; Table 2. The differences between the investigated treatments for C_{max} (ANOVA; $P < 0.05$) and T_{max} (Mann–Whitney U) were proved to be statistically significant. Interestingly, the $MRT_{(0-\infty)}$ of CHL was prolonged from 2.51 ±0.19 h, with the aqueous suspension, to 6.72 ±1.49 h with SXN4. This difference was proved to be statistically significant ($P< 0.05$).

The GR plasma concentration – time curves following oral administration of the aqueous drug solution and SXN4 in fasted rats were portrayed in Figure 6B. Like CHL profiles, the plasma profile of GR from SXN4 exhibited a higher C_{max} and a more prolonged $MRT_{(0-\infty)}$. The respective C_{max} estimates were 10.90 ±1.11 ng/mL and 8.10 ±1.23ng/mL, while the respective $MRT_{(0-\infty)}$ were found to be 9.39 ±1.94 h and 4.57 ±0.94h. Unlike CHL profiles, a longer median T_{max} value was revealed from SXNs (3 h vs 2h); Table 2. Statistically significant differences were revealed between the two treatments for C_{max}, $MRT_{(0-\infty)}$ and T_{max}.

It is worth to note that attainment of the T_{max} values of CHL and GR within 2–3 hrs post-dosing should point out the capability of SXN4 in offering chemotherapy with minimum potential for initiating nausea and/or vomiting.

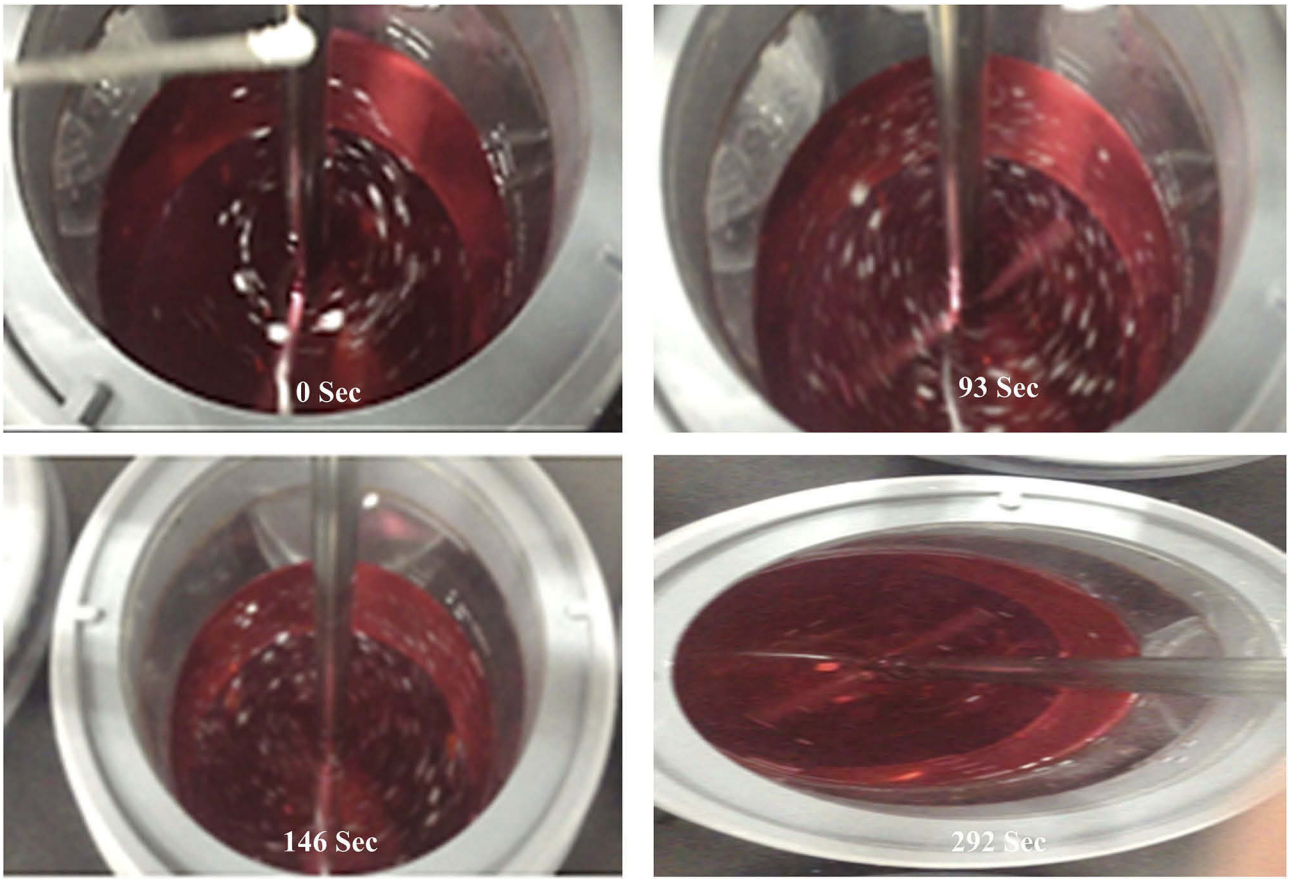

Figure 5 Photographs taken before and during in vitro wetting and floating studies of (GR/CHL)-loaded SXN4 showing the wetting time in 0.1 N HCl at 37 ± 0.5°C.

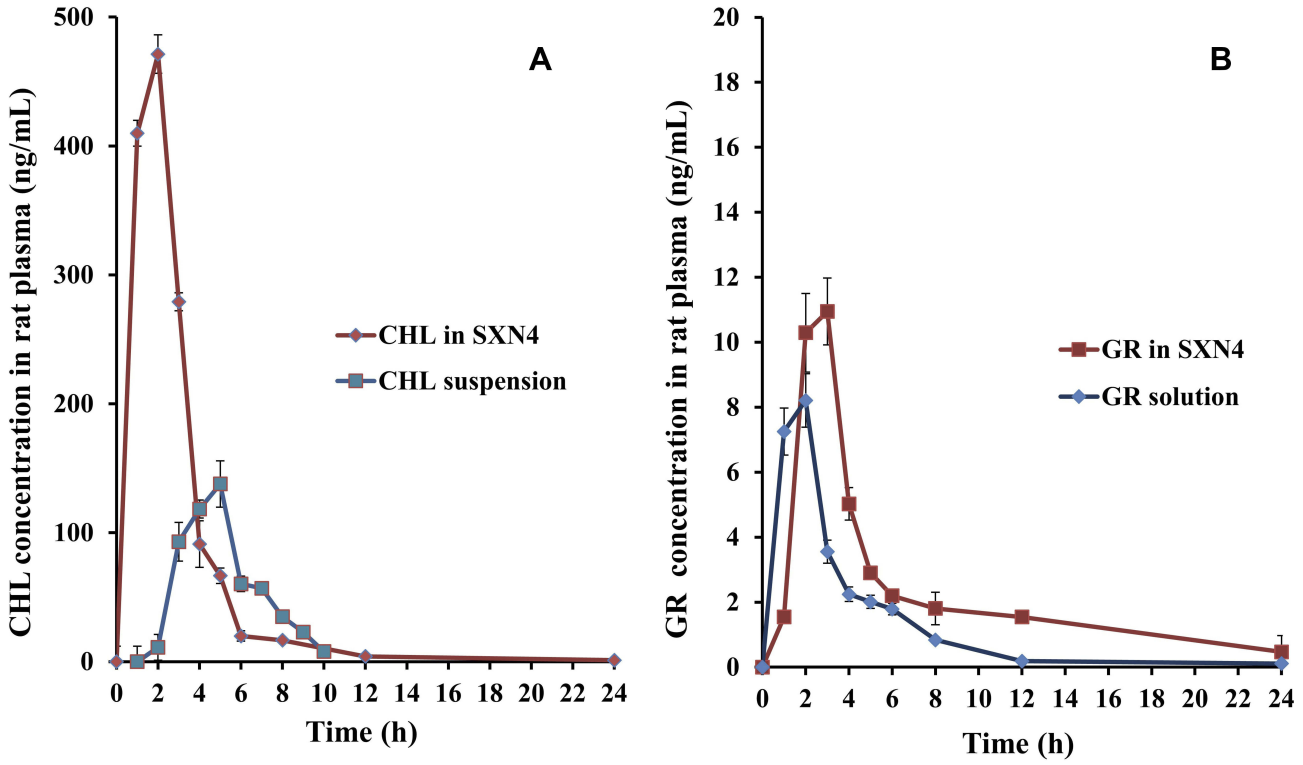

Figure 6 (**A**) Plasma concentration-time curves of CHL from SXN4 and an aqueous CHL suspension following oral administration in fasted rats at 4 mg/mL doses, mean ± S.D., n = 6. (**B**) Plasma concentration-time curves of GR from SXN4 and an aqueous GR solution following oral administration in fasted rats at 2 mg/mL doses, mean ± S.D., n = 6.

Compared to CHL suspension, the increase in the relative oral bioavailability of CHL from SXN4 was 1.75 folds. In a parallel line, the increase in the oral bioavailability of GR from SXN4, relative to GR solution, was 1.78 folds. The increases in the oral bioavailability of the loaded drugs could be related to different reasons, including; (i) the magnified hydrolytic stability of CHL in the gastric fluids, (ii) the enhancement in the dissolution rate as well as (iii) the prolonged circulation time and the slower opsonization rates because of the size and charge of SXNs. Xerogel nanoparticles interact with the plasma membrane via non-specific binding forces and then are endocytosed or penetrate the cellular membrane.[42] As mentioned earlier, nanoparticles are often engulfed via endocytosis and are then transferred to lysosomes; allowing for drug(s) release. Besides, the tumor microenvironment exhibits a low pH (due to hypoxia) and therefore, the drug release can be facilitated at the target site.[43]

Conclusions and Future Perspectives

TEOS-based spray dried SXNs incorporating GR and CHL were successfully developed, according to the central composite design, in a two-step sol-gel process. Based on the statistical evaluation of the results of the in vitro

Table 2 The Estimated Pharmacokinetic Parameters of GR and CHL Following Oral Administration of SXN4 and an Aqueous CHL Suspension Containing GR in Fasted Rats (Mean ± S.D., n = 6)

Pharmacokinetic Parameters	CHL		GR	
	Suspension	SXN4	Solution	SXN4
C_{max} (ng/mL)	137.82 ± 15.17	682.51 ± 22.37	8.10 ± 1.23	10.90 ± 1.11
*T_{max} (h)	4 (2–4)	2 (1.5–3)	2 (1–2)	3 (1–3)
$MRT_{(0-\infty)}$(h)	2.51 ± 0.19	6.72 ± 1.49	4.57 ± 0.94	9.39 ± 1.94
$AUC_{(0-24)}$ (ng·h/mL)	816.7 ± 20.14	1435.35 ± 19.52	30.65 ± 9.75	54.59 ± 14.29
$AUC_{(0-\infty)}$ (ng·h/mL)	905.1 ± 22.62	1442.15 ± 32.76	32.31 ± 8.64	60.23 ± 4.97

Note: *Median (range).

characterization studies and the in vivo pharmacokinetic studies, one promising gastroretentive system (SXN4) was proved to overcome most of the limitations of the loaded drugs, to improve their oral bioavailabilities and to prolong their circulation times. Further clinical studies are needed to explore the capability of this system in offering chemotherapy with minimum potential for initiating nausea and/or vomiting.

Disclosure

The authors report no conflicts of interest in this work.

References

1. Buckstein R, Kerbel R, Cheung M, et al. Lenalidomide and metronomic melphalan for CMML and higher risk MDS: a phase 2 clinical study with biomarkers of angiogenesis. *Leuk Res*. 2014;38(7):756–763. doi:10.1016/j.leukres.2014.03.022
2. Chaiyasat P, Chaiyasat A, Boontung W, Promdsorn S, Thipsit S. Preparation and characterization of poly(divinylbenzene) microcapsules containing octadecane. *Mater Sci Appl*. 2011;02(08):1007–1013.
3. Fu YJ, Mi FL, Wong TB, Shyu SS. Characteristic and controlled release of anticancer drug loaded poly (D,L-lactide) microparticles prepared by spray drying technique. *J Microencapsul*. 2001;18(6):733–747. doi:10.1080/02652040010055649
4. Tadros MI, Al-Mahallawi AM. Long-circulating lipoprotein-mimic nanoparticles for smart intravenous delivery of a practically-insoluble antineoplastic drug: development, preliminary safety evaluations and preclinical pharmacokinetic studies. *Int J Pharm*. 2015;493(1–2):439–450. doi:10.1016/j.ijpharm.2015.08.011
5. Thirumaran R, Prendergast GC, Gilman PB. Cytotoxic chemotherapy in clinical treatment of cancer. *Cancer Immunother*. 2007;101–116.
6. Roscoe JA, Morrow GR, Hickok JT, Stern RM. Nausea and vomiting remain a significant clinical problem: trends over time in controlling chemotherapy-induced nausea and vomiting in 1413 patients treated in community clinical practices. *J Pain Symptom Manage*. 2000;20(2):113–121. doi:10.1016/S0885-3924(00)00159-7
7. Ballatori E, Roila F. Impact of nausea and vomiting on quality of life in cancer patients during chemotherapy. *Health Qual Life Outcomes*. 2003;1:46. doi:10.1186/1477-7525-1-46
8. Farrell C, Brearley SG, Pilling M, Molassiotis A. The impact of chemotherapy-related nausea on patients' nutritional status, psychological distress and quality of life. *Support Care Cancer*. 2013;21(1):59–66. doi:10.1007/s00520-012-1493-9
9. Roila F, Warr D, Aapro M, et al. Delayed emesis: moderately emetogenic chemotherapy (Single-day chemotherapy regimens only). *Support Care Cancer*. 2011;Suppl 1:S57–S62. doi:10.1007/s00520-010-1039-y
10. Kalia V, Garg T, Rath G, Goyal AK. Development and evaluation of a sublingual film of the antiemetic granisetron hydrochloride. *Artif Cells Nanomedicine Biotechnol*. 2016;44(3):842–846.
11. Brayfield A, ed. *Martindale: The Complete Drug Reference*. 38th ed. London: The Pharmaceutical Press; 2014.
12. Stankus T. Drugs and poisons. *Serials Librarian*. 1996;27:87–102. doi:10.1300/J123v27n02_07
13. Kim JJ, Tannock IF. Repopulation of cancer cells during therapy: an important cause of treatment failure. *Nat Rev Cancer*. 2005;5(7):516–525. doi:10.1038/nrc1650
14. Kerbel RS, Klement G, Pritchard KI, Kamen B. Continuous low-dose anti-angiogenic/metronomic chemotherapy: from the research laboratory into the oncology clinic. *Ann Oncol*. 2002;13(1):12–15. doi:10.1093/annonc/mdf093
15. Browder T, Butterfield CE, Kräling BM, et al. Antiangiogenic scheduling of chemotherapy improves efficacy against experimental drug-resistant cancer. *Cancer Res*. 2000;60(7):1878–1886.
16. Croissant JG, Cattoën X, et al. Syntheses and applications of periodic mesoporous organosilica nanoparticles. *Nanoscale*. 2015;7(48):20318–20334. doi:10.1039/C5NR05649G
17. Croissant JG, Fatieiev Y, Almalik A, Khashab NM. Mesoporous silica and organosilica nanoparticles: physical chemistry, biosafety, delivery strategies, and biomedical applications. *Adv Healthc Mater*. 2018;7(4):1700831.
18. Huang WF, Tsui GCP, Tang CY, Yang M. Optimization strategy for encapsulation efficiency and size of drug loaded silica xerogel/polymer core-shell composite nanoparticles prepared by gelation-emulsion method. *Polym Eng Sci*. 2018;58(5):742–751. doi:10.1002/pen.24609
19. Zhai W, He C, Wu L, et al. Degradation of hollow mesoporous silica nanoparticles in human umbilical vein endothelial cells. *J Biomed Mater Res - Part B Appl Biomater*. 2012;100 B(5):1397–1403. doi:10.1002/jbm.b.32711
20. Ekkapongpisit M, Giovia A, Follo C, Caputo G, Isidoro C. Biocompatibility, endocytosis, and intracellular trafficking of mesoporous silica and polystyrene nanoparticles in ovarian cancer cells: effects of size and surface charge groups. *Int J Nanomedicine*. 2012;7:4147–4158. doi:10.2147/IJN.S33803
21. Chatterji DC, Yeager RL, Gallelli JF. Kinetics of chlorambucil hydrolysis using high-pressure liquid chromatography. *J Pharm Sci*. 1982;71(1):50–54. doi:10.1002/jps.2600710113
22. Antovska P, Cvetkovska M, Goračinova K. Preparation and characterization of sol-gel processed spray dried silica xerogel microparticles as carriers of heparin sodium. *Bull Chem Technol Macedonia*. 2006;25(2):121–126.
23. Levy MY, Benita S. Drug release from submicronized o/w emulsion: a new in vitro kinetic evaluation model. *Int J Pharm*. 1990;66(1–3):29–37. doi:10.1016/0378-5173(90)90381-D
24. Zhuang CY, Li N, Wang M, et al. Preparation and characterization of vinpocetine loaded nanostructured lipid carriers (NLC) for improved oral bioavailability. *Int J Pharm*. 2010;394(1–2):179–185. doi:10.1016/j.ijpharm.2010.05.005
25. Bhardwaj U, Burgess DJ. A novel USP apparatus 4 based release testing method for dispersed systems. *Int J Pharm*. 2010;388(1–2):287–294. doi:10.1016/j.ijpharm.2010.01.009
26. Tadros MI, Fahmy RH. Controlled-release triple anti-inflammatory therapy based on novel gastroretentive sponges: characterization and magnetic resonance imaging in healthy volunteers. *Int J Pharm*. 2014;472(1–2):27–39. doi:10.1016/j.ijpharm.2014.06.013
27. Washburn EW. Note on a method of determining the distribution of pore sizes in a porous material. *Proc Natl Acad Sci USA*. 1921;7(4):115–116. doi:10.1073/pnas.7.4.115
28. Orlu M, Cevher E, Araman A. Design and evaluation of colon specific drug delivery system containing flurbiprofen microsponges. *Int J Pharm*. 2006;318(1–2):103–117. doi:10.1016/j.ijpharm.2006.03.025
29. Song H, Nie S, Yang X, et al. Characterization and in vivo evaluation of novel lipid-chlorambucil nanospheres prepared using a mixture of emulsifiers for parenteral administration. *Int J Nanomedicine*. 2010;5(1):933–942. doi:10.2147/IJN.S14596
30. Danks AE, Hall SR, Schnepp Z. The evolution of "sol-gel" chemistry as a technique for materials synthesis. *Mater Horizons*. 2016;3(2):91–112. doi:10.1039/C5MH00260E
31. Elsagh A. Synthesis of silica nanostructures and optimization of their size and morphology by use of changing in synthesis conditions. *E-Journal Chem*. 2012;9(2):659–668. doi:10.1155/2012/109765
32. Kortesuo P, Ahola M, Kangas M, Yli-Urpo A, Kiesvaara J, Marvola M. In vitro release of dexmedetomidine from silica xerogel monoliths: effect of sol-gel synthesis parameters. *Int J Pharm*. 2001;221(1–2):107–114. doi:10.1016/S0378-5173(01)00656-1

33. Kortesuo P, Ahola M, Kangas M, et al. Effect of synthesis parameters of the sol–gel-processed spray-dried silica gel microparticles on the release rate of dexmedetomidine. *Biomaterials*. 2002;23(13):2795–2801. doi:10.1016/S0142-9612(02)00016-9
34. Kesmez Ö, Burunkaya E, Kiraz N, Çamurlu HE, Asiltürk M, Arpaç E. Effect of acid, water and alcohol ratios on sol-gel preparation of antireflective amorphous SiO_2 coatings. *J Non Cryst Solids*. 2011;357(16–17):3130–3135. doi:10.1016/j.jnoncrysol.2011.05.003
35. Maeda H, Matsumura Y. Tumoritropic and lymphotropic principles of macromolecular drugs. *Crit Rev Ther Drug Carrier Syst*. 1989;6(3):193–210.
36. Yuan F, Dellian M, Fukumura D, et al. Vascular permeability in a human tumor xenograft: molecular size dependence and cutoff size. *Cancer Res*. 1995;55(17):3752–3756.
37. Seleem MN, Munusamy P, Ranjan A, Alqublan H, Pickrell G, Sriranganathan N. Silica-antibiotic hybrid nanoparticles for targeting intracellular pathogens. *Antimicrob Agents Chemother*. 2009;53(10):4270–4274. doi:10.1128/AAC.00815-09
38. International Agency for Research on Cancer. IARC monographs on the evaluation of carcinogenic risks to humans. *IARC Monogr Eval Carcinog Risks to Humans*. 2010;93:9–38.
39. Wang X, Cao Y, Yan H. Chlorambucil loaded in mesoporous polymeric microspheres as oral sustained release formulations with enhanced hydrolytic stability. *Mater Sci Eng C*. 2018;91:564–569. doi:10.1016/j.msec.2018.05.078
40. Van Speybroeck M, Barillaro V, Do TT, et al. Ordered mesoporous silica material SBA-15: a broad-spectrum formulation platform for poorly soluble drugs. *J Pharm Sci*. 2009;98(8):2648–2658. doi:10.1002/jps.21638
41. Abd-Elbary A, Tadros MI, Alaa-Eldin AA. Sucrose stearate-enriched lipid matrix tablets of etodolac: modulation of drug release, diffusional modeling and structure elucidation studies. *AAPS PharmSciTech*. 2013;14(2):656–668. doi:10.1208/s12249-013-9951-3
42. Nel AE, Mädler L, Velegol D, et al. Understanding biophysicochemical interactions at the nano-bio interface. *Nat Mater*. 2009;8(7):543–557. doi:10.1038/nmat2442
43. Gatenby RA, Gillies RJ. Why do cancers have high aerobic glycolysis? *Nat Rev Cancer*. 2004;4(11):891–899. doi:10.1038/nrc1478